ISBN: 978-3-95450-262-2 ISSN: 2673-5350 doi: 10.18429/JACoW-IBIC2025-WEPMO28

# OPTIMISATION OF A FIBRE-BASED TWO-COLOUR BALANCED OPTICAL CROSS-CORRELATOR*

J. Christie† [1], L. Corner[1], The University of Liverpool, Liverpool, U.K.
E. W. Snedden, ASTeC, STFC Daresbury Laboratory, UK
J. R. Henderson, Coherent Scotland Ltd, Glasgow, UK
[1]also at The Cockcroft Institute, Daresbury, UK

*Abstract*

As part of the ongoing Full Energy Beam Exploitation (FEBE) upgrade to the Compact Linear Accelerator for Research and Applications (CLARA) at the Daresbury Laboratory, UK, few-femtosecond optical synchronisation between the new Ti:Sapphire terawatt FEBE laser and the Er:Yb optical master oscillator (OMO) is required for user experiments. To achieve this, a fibre-based two-colour balanced optical cross-correlator (BOXC) using waveguided periodically-poled lithium niobate (PPLN) crystals is being developed. A fibre-based BOXC could have greater sensitivity to timing jitter between two lasers than traditional free-space devices. In this manuscript, the design of the fibre-based two-colour BOXC is presented. The effect of pulse chirp on the sensitivity of the BOXC is investigated, and plans for optimising the design of the BOXC are discussed along with plans for integrating the fibre-based BOXC into the optical synchronisation network at Daresbury.

## INTRODUCTION

The Compact Linear Accelerator for Research and Applications (CLARA) is an electron accelerator based in Daresbury Laboratory, UK, that serves as a user facility for academia and industry. At the time of writing, CLARA is undergoing commissioning of its Phase 2 upgrade, with the goal of generating 250 MeV electron bunches with a maximum bunch charge of 250 pC at 100 Hz [1]. Part of the Phase 2 upgrade is the Full Energy Beam Exploitation (FEBE) beamline, a dedicated user experimental area where 100 TW pulses from the new Ti:Sapphire FEBE laser can co-propagate and interact with the 250 MeV electron bunches from CLARA. Having access to high-power laser pulses and mid-energy electron bunches in the same experimental area will enable further research into novel acceleration techniques such as laser and plasma wakefield acceleration. However, such experiments will require femtosecond-level synchronisation of the FEBE laser to the Er:Yb optical master oscillator (OMO) for sufficient temporal resolution [2].

To achieve the required synchronisation performance between the FEBE laser and the OMO, a fibre-based two-colour balanced optical cross-correlator (BOXC) is being developed at Daresbury. A BOXC determines the timing delay between two laser pulses via sum-frequency generation (SFG) in a nonlinear crystal. However, many existing two-colour BOXCs utilise bulk free-space nonlinear crystals [3], limiting their long-term stability due to environmental factors affecting the alignment of the free-space optics. A fibre-based two-colour BOXC would remove the need for most free-space optics, potentially improving the stability of the BOXC. However, dispersion from the fibre components in the BOXC will cause the laser pulses to broaden in time, which could affect the BOXC performance due to reduced sum-frequency conversion.

In our previous work, a proof-of-concept fibre-based two-colour BOXC with a sensitivity of 0.971 mV/fs was demonstrated [4]. Here, we are looking to optimise the performance of the fibre-based BOXC by investigating the effect of fibre dispersion on sum-frequency generation. This will allow for the generation of more intense sum-frequency radiation for the same input laser power, thus making the BOXC more sensitive to laser pulse arrival time fluctuations.

## FIBRE-BASED TWO-COLOUR BOXC

The layout of the fibre-based two-colour BOXC is shown in Fig. 1; a detailed description of the layout is provided in [5]. The BOXC uses two 5 mm-long, type-0 phase-matched, periodically poled $LiNbO_3$ (PPLN) crystal waveguides, chosen for its large effective nonlinear coefficient of $d_{\text{eff}}$ = 16.1 pm/V [6]. The implemented ridge waveguide also increases the interaction length by reducing laser pulse diffraction within the crystal, leading to increased conversion efficiency compared to bulk-optic crystals.

The Origami-15 OMO, which operates at 249.875 MHz, supplies 1560 nm pulses to the BOXC via a stabilised fibre link. The pulses from the link, which have a full width half maximum (FWHM) spectral width of 10.9 nm and a FWHM pulse duration of 250 fs, are amplified by an erbium-doped fibre amplifier (EDFA) before distribution to the BOXC.

For testing the BOXC, 800 nm pulses are supplied by a Coherent Micra-5 laser system. The Micra-5 operates at 83.292 MHz and produces pulses with a FWHM spectral width of 27.4 nm and a measured FWHM pulse duration of 970 fs, much greater the bandwidth-limited duration of 24.5 fs due to dispersive optical elements within the beam transport to the BOXC.

After coupling and polarisation adjustment, the input pulses are split 50:50 and sent to the PPLN waveguides. The fibre delay stage imparts an additional time delay to one of the 1560 nm components, resulting in the sets of input pulses having different pulse delays. The two waveguides then generate 528.8 nm sum-frequency pulses with different

* Work supported by STFC grant no. ST/V001612/1
† J.S.Christie@liverpool.ac.uk

ISBN: 978-3-95450-262-2 ISSN: 2673-5350 doi: 10.18429/JACoW-IBIC2025-WEPMO28

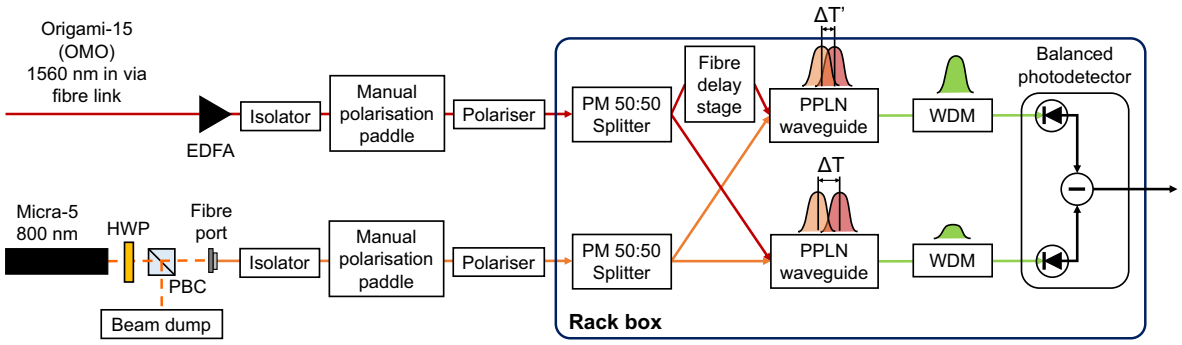


Figure 1: Layout of the fibre-based two-colour BOXC. EDFA: Erbium-doped fibre amplifier; HWP: Half-wave plate; PBC: Polarising beamsplitter cube; PM: Polarisation-maintaining; WDM: Wavelength division multiplexer; Rack box: 48.3 cm × 48.3 cm rack box housing a 39.4 cm × 40.6 cm optical breadboard.

intensities due to the different temporal overlaps of the input pulses, and the difference in the two voltage responses is taken. Scanning over the input pulse delay gives a voltage error signal that is linearly proportional to the pulse delay, allowing for the detection of timing fluctuations much shorter than the pulse duration. This signal can be used to adjust the cavity length and hence repetition rate of the Micra-5, with the aim of keeping the error signal locked to the zero-crossing point, resulting in the synchronisation of the Micra-5 to the OMO pulse train.

## EFFECT OF DISPERSION ON SUM-FREQUENCY GENERATION

In this version of the BOXC design, the 800 nm pulses travel through 8.7 m of single-mode fibre and the 1560 nm pulses travel through approximately 32.1 m of single-mode fibre and 3.0 m of erbium-doped fibre from the EDFA. Owing to their large spectral widths, the pulses undergo significant temporal broadening as a result of fibre dispersion, with the 800 nm pulses broadening from 970 fs to 39 ps and the 1560 nm pulses broadening from 250 fs to 3.9 ps.

The group delay dispersion (GDD) gained by the pulse from fibre dispersion can be found from the expression

$$\tau = \tau_0 \sqrt{1 + \left(4 \ln 2 \frac{\mathrm{GDD}}{\tau_0^2}\right)^2}, \qquad (1)$$

where $\tau$ is the stretched pulse duration after the fibre and $\tau_0$ is the bandwidth-limited pulse duration. Thus, the GDDs gained by the 800 nm and 1560 nm pulse are $3.5 \times 10^5$ fs$^2$ and $-3.5 \times 10^5$ fs$^2$ respectively; note that the GDDs have opposite signs as the dispersion parameter of the 800 nm fibre is negative [7], whereas the 1560 nm fibre dispersion parameter is positive [8]. The fibre also imparts a linear frequency chirp $b$ to each pulse, given by

$$b = \frac{4(\mathrm{GDD})}{2\pi(4(\mathrm{GDD})^2 + (\tau_0^2/(2\ln 2))^2)} \approx \frac{1}{2\pi(\mathrm{GDD})}. \qquad (2)$$

Thus, the respective linear chirps of the 800 nm and 1560 nm pulses are 0.45 THz/ps and −0.45 THz/ps.

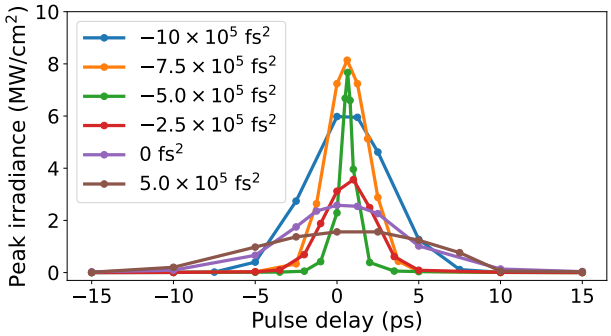


Figure 2: Plot of peak sum-frequency irradiance against pulse delay for different values of the 1560 nm group delay dispersion (GDD).

Because both pulses entering the nonlinear crystal have linear chirp, the resulting sum-frequency pulse will also have a linear chirp $b_{SFG} = b_{800} + b_{1560}$, giving the sum-frequency pulse a time-dependent instantaneous frequency of $\omega(t) = \omega_{SFG} + b_{SFG}t$, where $\omega_{SFG}$ is the SFG centre frequency. Due to the phase-matching condition of the nonlinear crystal, which requires the frequency shift $\Delta\omega = \omega(t) - \omega_{SFG} \approx 0$, the chirps of the input pulses can be used to alter the instantaneous frequency of the sum-frequency pulse so that the phase-matching condition is no longer satisfied. As a result, the sum-frequency interaction can be limited to a small portion of the pulse bandwidth where the phase-matching condition is satisfied [9], allowing for the generation of cross-correlation traces much narrower than the input pulse durations.

This effect can be seen in Fig. 2, where SNLO is used to simulate the SFG process within the PPLN waveguide [10]. Here, the 800 nm pulse GDD is kept constant at $3.5 \times 10^5$ fs$^2$, and the 1560 nm pulse GDD is varied from $5.0 \times 10^5$ fs$^2$ to $-10 \times 10^5$ fs$^2$. By measuring the peak sum-frequency irradiance for a given 1560 nm pulse GDD over a range of pulse delays, cross-correlations traces can be generated for various 1560 nm pulse GDDs. Note that the pulse delay is defined to be positive when the 1560 nm pulse is trailing the 800 nm pulse.

ISBN: 978-3-95450-262-2 ISSN: 2673-5350 doi: 10.18429/JACoW-IBIC2025-WEPMO28

Table 1: Average Laser Powers

| Wavelength (nm) | Avg. power, delay stage PPLN (mW) | Avg. power, undelayed PPLN (mW) |
|---|---|---|
| 1560 | 5.3(1) | 4.3(1) |
| 800.0 | 3.5(1) | 1.8(1) |

When both pulses have positive GDD and thus positive chirp, $\omega(t)$ changes very quickly due to the large chirp of the sum-frequency pulse. Thus, $\omega(t)$ only satisfies $\Delta\omega \approx 0$ for a short length of time, resulting in reduced peak sum-frequency irradiance and cross-correlation signal amplitude. Additionally, due to the temporal walkoff of the pulses within the crystal, the input pulses will scan over the entire region where $\Delta\omega \approx 0$ for a large range of pulse delays, resulting in sum-frequency generation at large pulse delays and a wider cross-correlation signal.

As the 1560 nm pulse GDD decreases and becomes more negative, the chirp of the sum-frequency pulse also decreases in magnitude. At small pulse delays, $\Delta\omega \approx 0$ is satisfied over a greater length within the crystal due to $\omega(t)$ changing more slowly, resulting in increasing cross-correlation signal amplitude. The slower change in $\omega(t)$ also leads to reduced sum-frequency generation at large pulse delays due to poor phase-matching, leading to narrower cross-correlation traces. As the 1560 nm pulse GDD decreases further, the cross-correlation trace width increases and the maximum peak irradiance starts to decrease due to depletion of the 1560 nm pulse as it becomes broader in time and thus less intense.

## BOXC PERFORMANCE

The simulation results suggest that, due to the large positive GDD of the 800 nm pulse, the cross-correlation trace intensity increases with increasingly negative 1560 nm pulse GDD up to a GDD of around $-5.0 \times 10^5$ fs$^2$. To investigate the effect of pulse GDD on the BOXC sensitivity, extra 1560 nm fibre up to 8 m in length is added to the BOXC to vary the 1560 nm pulse GDD between $-3.5 \times 10^5$ fs$^2$ and $-5.4 \times 10^5$ fs$^2$. After ensuring the 1560 nm and 800 nm average powers at the PPLN waveguides are constant, the BOXC error signal is obtained for each 1560 nm fibre length by introducing a small frequency offset between the Micra-5 and the OMO to slowly scan the pulse trains over one another; a detailed explanation of the method can be found in Ref. [5]. Table 1 gives the average powers of the 1560 nm and 800 nm pulses entering each PPLN waveguide.

Figure 3(a) shows how the BOXC error signal changes with increasing 1560 nm fibre. As the 1560 nm GDD becomes increasingly negative, the amplitude of the cross-correlation traces increases and the FWHM of the traces decreases, as predicted by Fig. 2, leading to increased BOXC sensitivity. The maximum sensitivity occurs with 8 m of additional fibre, corresponding to a 1560 nm GDD of $-5.4 \times 10^5$ fs$^2$ in agreement with the simulation results.

Figure 3(b) shows the BOXC error signal and the cross-correlation traces with 8 m of additional 1560 nm fibre. The

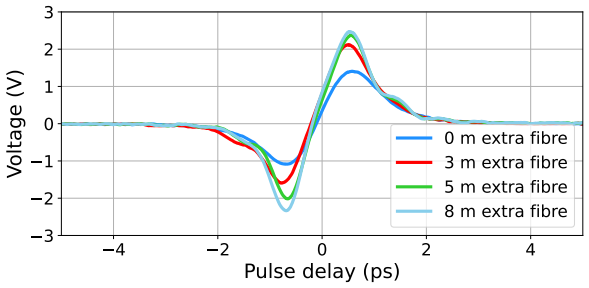


(a)

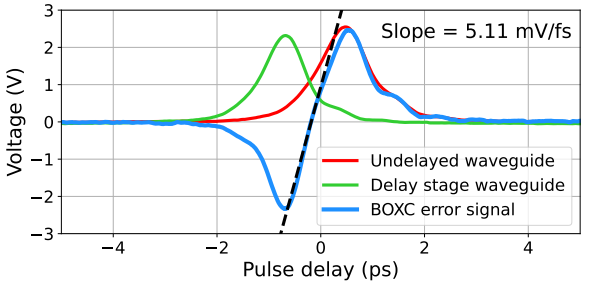


(b)

Figure 3: (a) Effect of increasing 1560 nm single-mode fibre length on the BOXC voltage error signal. (b) BOXC error signal with 8 m of additional 1560 nm single-mode fibre.

measured sensitivity is 5.11 mV/fs, 5 times higher than comparable bulk-optic two-colour BOXCs after accounting for transimpedance gain and photodetector responsivity [3].

## CONCLUSION

The effect of fibre dispersion on the performance of a fibre-based two-colour BOXC was investigated. Due to the large positive chirp of the 800 nm pulse from fibre dispersion, it was found in both simulations and experiments that increasing the negative GDD of the 1560 nm pulse by adding additional single-mode fibre increased the peak cross-correlation trace voltage and the sensitivity of the BOXC. Using these findings, a maximum BOXC sensitivity of 5.11 mV/fs was achieved, 5 times greater than comparable bulk-optic BOXCs.

To investigate how the 800 nm pulse GDD affects the BOXC, an 800 nm pulse compressor is being constructed to allow for adjustment of the 800 nm pulse GDD and to compensate for fibre dispersion. Future investigation of the performance of the two-colour fully fibre-coupled BOXC will involve measuring the environmental stability of the BOXC sensitivity, using the BOXC error signal to lock the Micra-5 to the OMO, and measuring the resulting integrated timing jitter and long-term stability.

## ACKNOWLEDGEMENTS

This work was supported by the Science and Technology Facilities Council under grant ST/V001612/1 and by the studentship project 2489637.

ISBN: 978-3-95450-262-2 ISSN: 2673-5350 doi: 10.18429/JACoW-IBIC2025-WEPMO28



# REFERENCES


[1] D. Angal-Kalinin, AR. Bainbridge, JK. Jones, TH. Pacey, YM. Saveliev, and EW. Snedden, "The design of the Full Energy Beam Exploitation (FEBE) beamline on CLARA", in *Proc. LINAC'22*, Liverpool, UK, Aug.–Sep. 2022, pp. 585–588. doi:10.18429/JACoW-LINAC2022-TUPORI18

[2] A. JW. Reitsma, R. A. Cairns, R. Bingham, and D. A. Jaroszynski, "Efficiency and energy spread in laser-wakefield acceleration", *Phys. Rev. Lett.*, vol. 94, no. 8, pp. 1–4, 2005. doi:10.1103/PhysRevLett.94.085004

[3] C. L. Li, L. Feng, B. Liu, J. G. Wang, X. T. Wang, and W. Y. Zhang, "Two color balanced optical cross correlator to synchronize distributed lasers for SHINE project", in *Proc. IBIC'21*, Pohang, Korea, Sep. 2021, pp. 370–372. doi:10.18429/JACoW-IBIC2021-WEPP05

[4] J. Christie, L. Corner, J. R. Henderson, and E. W. Snedden, "Developing a two-colour all-fibre balanced optical cross-correlator for sub-femtosecond synchronisation", in *Proc. IPAC'23*, Venice, Italy, May 2023, pp. 4135–4138. doi:10.18429/JACoW-IPAC2023-THPA073

[5] J. Christie, J. R. Henderson, E. W. Snedden, and L. Corner, "Two-colour balanced optical cross-correlator using fibre-coupled PPLN waveguides", *Opt. Contin.*, vol. 4, no. 7, pp. 1443–1457, Jul. 2025. doi:10.1364/OPTCON.551610

[6] HC Photonics, PPLN Guide: Overview, Jun. 2017. https://www.hcphotonics.com/ppln-guide-overview

[7] Coherent, 780-HP Dispersion. https://www.coherent.com/resources/application-note/components-and-accessories/specialty-optical-fibers/780-hp-dispersion.pdf

[8] Thorlabs, SMF-28-100 Spec Sheet, Nov. 2015. https://www.thorlabs.com/thorproduct.cfm?partnumber=smf-28-100

[9] F. Raoult *et al.*, "Efficient generation of narrow-bandwidth picosecond pulses by frequency doubling of femtosecond chirped pulses", *Opt. Lett.*, vol. 23, no. 14, pp. 1117–1119, Jul. 1998. doi:10.1364/OL.23.001117

[10] AS-Photonics, SNLO Classic (Free Version), Feb. 2023. https://as-photonics.com/products/snlo/